

# Spectroscopic Ellipsometric Study of ZnO and Zn<sub>1-x</sub>Mg<sub>x</sub>O Thin Films Grown on (0001) Sapphire Substrate

T. D. KANG and Hosun LEE\*

*Department of Physics, Institute for Natural Sciences, Kyung Hee University, Suwon 449-701*

Won-Il PARK and Gyu-Chul Yi

*Department of Materials Science and Engineering,  
Pohang University of Science and Technology, Pohang 790-784*

(Received 7 August 2003)

We grew ZnO and Zn<sub>1-x</sub>Mg<sub>x</sub>O thin films on (0001) sapphire substrates by using metal-organic vapor phase epitaxy and measured the pseudo-dielectric functions using variable-angle spectroscopic ellipsometry. We analyzed the pseudo-dielectric functions by using the multi-layer model. The dielectric functions were fitted by using a Holden model dielectric function. We used anisotropic layer modeling for the ZnO thin film, whereas we adopted the approximation of isotropic layer modeling for the Zn<sub>1-x</sub>Mg<sub>x</sub>O alloys. We also discuss the Mg composition dependence of the band-gap and the binding energy in Zn<sub>1-x</sub>Mg<sub>x</sub>O alloys, and consider the valence-band ordering in ZnO thin films.

PACS numbers: 78.20.Ci, 78.40.Fy, 78.66.Hf, 71.20.Nr

Keywords: ZnO, Dielectric function, Ellipsometry, Critical point, Holden model

## I. INTRODUCTION

ZnO is a II-VI semiconductor with a large band gap ( $\sim 3.4$  eV) [1]. The ZnO crystal has a wurtzite structure, and the optical function shows uniaxial behavior. For ZnO grown on (0001) sapphire, the optic axis is along the growth direction [denoted as the *c* axis], *i.e.*, the surface normal direction. An MgO crystal, one of the endpoint binaries of Zn<sub>1-x</sub>Mg<sub>x</sub>O, has a cubic structure like NaCl, and the optical function is isotropic. The wide band-gap ZnO and Zn<sub>1-x</sub>Mg<sub>x</sub>O semiconductors possess attractive properties for applications in optoelectronic and display devices because of their wide range luminescence from blue to ultraviolet and because of their large exciton binding energy ( $\sim 60$  meV) [2, 3]. The fundamental band-gap energy of Zn<sub>1-x</sub>Mg<sub>x</sub>O can be varied from 3.4 eV to 7.6 eV by alloying ZnO with MgO, and depends on the Mg content [4]. The ordering of the valence band is controversial and has not been settled yet. The anisotropic dielectric function of bulk ZnO has been reported by researchers, whereas that of the ZnO thin film grown on sapphire has not been reported so far [5, 6]. Only approximate isotropic dielectric functions of thin-film ZnO grown on (0001) Al<sub>2</sub>O<sub>3</sub> have been reported [1, 7, 8].

In this work, we grew ZnO and Zn<sub>1-x</sub>Mg<sub>x</sub>O thin films

by using metal-organic vapor phase epitaxy (MOVPE) system. Pseudo-dielectric functions were measured by variable angle spectroscopic ellipsometry (SE) [5, 7]. We determined the uniaxial dielectric function of ZnO thin films and the isotropic dielectric function of Zn<sub>1-x</sub>Mg<sub>x</sub>O thin films grown on (0001) sapphire by using a Holden model dielectric function (MDF) [6, 9].

## II. EXPERIMENT

ZnO and Zn<sub>1-x</sub>Mg<sub>x</sub>O ( $x = 0.2, 0.8$ ) films were grown on Al<sub>2</sub>O<sub>3</sub> (0001) substrates by using MOVPE. Before the Zn<sub>1-x</sub>Mg<sub>x</sub>O films were grown, thin ZnO buffer layers were grown, which significantly improved the crystallinity of the Zn<sub>1-x</sub>Mg<sub>x</sub>O films [4]. The Mg content was determined using a combination of absorption, photoluminescence (PL), inductively coupled plasma optical emission spectroscopy, and X-ray diffraction. SE measurements were performed at room temperature with a rotating-analyzer ellipsometer (Woollam Inc., VASE model) in the 1.0 - 6.0 eV energy range at intervals of 0.02 eV. All the spectra were taken at an angle of incidence of 65° or 70° and were measured with high accuracy by using an auto-retarder. Single-sided polished substrates with roughened back surfaces were used to reduce back reflection. X-ray diffraction showed some degree of residual strain in the thin films, which was due to the large

\*E-mail: hlee@khu.ac.kr

lattice mismatch ( $\sim 32\%$ ).

The measured ellipsometric data were represented in the form of the ellipsometric parameters  $\Psi$  and  $\Delta$ , which are related to the relative reflectance ratio  $\rho = r_p/r_s$ . The parameter  $\rho = \tan(\Psi) \exp(i\Delta)$  can be converted to pseudo-dielectric functions very easily. We determined the dielectric functions of ZnO and  $\text{Zn}_{1-x}\text{Mg}_x\text{O}$  layers through multi-layer modeling using a linear regression analysis (LRA) and a Holden MDF. We included surface roughness by using the effective medium approximation (EMA) and by assuming a mixture of voids with the top layer [1,6].

### III. RESULTS AND DISCUSSION

The strong excitonic properties of the  $E_0$  gap significantly modify the dielectric functions near the  $E_0$  gap in ZnO [10]. This phenomenon is typical in II-VI semiconductors, which have strongly ionic characteristics, in general. Using a Lorentzian approximation for the line-shape broadening of both the excitonic states and the band edge, Holden and coworkers used five parameters to derive the dielectric function near a 3-D critical point (CP) modified by excitonic interactions [9]. The formula can be expressed as

$$\epsilon(E) = \frac{A}{2E^2} \sum_{n=1}^{\infty} [g_{b,n}(E + i\Gamma_n) - g_{b,n}(i\Gamma_n)] + g_u(E + i\Gamma_0) - g_u(i\Gamma_0), \quad (1)$$

$$g_{b,n}(\xi) = \frac{8R}{n^3} \left[ \frac{E_0 - \frac{R}{n^2}}{(E_0 - \frac{R}{n^2})^2 - \xi^2} \right], \quad (2)$$

$$g_u(\xi) = -\ln \left( \frac{E_0^2 - \xi^2}{R^2} \right) - \frac{1}{2} \sum_{n=1}^{\infty} g_{b,n}(\xi) - \pi \left[ \cot \left( \frac{\pi\sqrt{R}}{\sqrt{E_0 - \xi}} \right) + \cot \left( \frac{\pi\sqrt{R}}{\sqrt{E_0 + \xi}} \right) \right], \quad (3)$$

where the parameters are the amplitude  $A$ , the CP energy  $E_0$ , the excitonic binding energy  $R$ , the broadening of the bandgap  $\Gamma_0$ , and the broadening of the exciton  $\Gamma_0^{ex}$ . The energy and the broadening of the  $n$ -th exciton are given by

$$E_{n,0}^{ex} = E_0 - \frac{R}{n^2}, \quad (4)$$

$$\Gamma_n = \Gamma_0 - \frac{\Gamma_0 - \Gamma_0^{ex}}{n^2}. \quad (5)$$

To accommodate the contributions from the electronic transitions at energies above the experimental energy

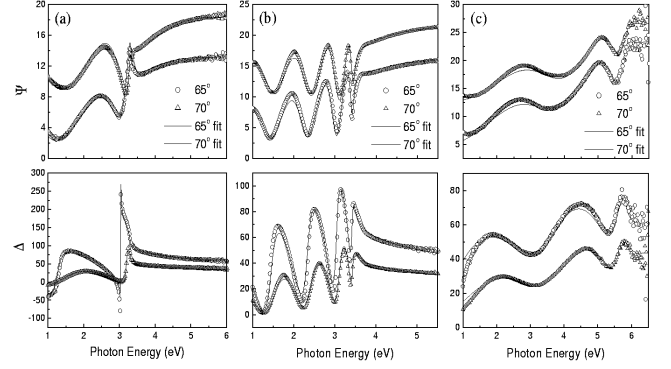


Fig. 1. Ellipsometric parameters  $\Psi$  and  $\Delta$  of (a) ZnO, (b)  $\text{Zn}_{0.8}\text{Mg}_{0.2}\text{O}$ , and (c)  $\text{Zn}_{0.2}\text{Mg}_{0.8}\text{O}$  thin films grown on (0001) sapphire and their curve fits.

Table 1. Fit parameters for bulk ZnO, thin-film ZnO, and thin-film  $\text{Zn}_{1-x}\text{Mg}_x\text{O}$ . The fit parameters are the amplitude ( $A$ ), the energy threshold ( $E_0$ ), the binding energy ( $R$ ), the broadening of the band gap ( $\Gamma_0$ ), and the broadening of the exciton of the  $E_0$  gap ( $\Gamma_0^{ex}$ ), respectively.

	$A$	$E_0$ (eV)	$R$ (meV)	$\Gamma_0$ (meV)	$\Gamma_0^{ex}$ (meV)
(ZnO bulk) $E_{\perp c}$	7.17	3.373	55.3	1.0	23.6
$E_{\parallel c}$	7.90	3.407	51.3	5.34	24.9
(ZnO film) $E_{\perp c}$	7.53	3.378	61.1	25.0	35.7
$E_{\parallel c}$	7.66	3.413	72.8	1.4	55.3
$\text{Zn}_{0.8}\text{Mg}_{0.2}\text{O}$ film	7.50	3.604	66.4	16.1	54.5
$\text{Zn}_{0.2}\text{Mg}_{0.8}\text{O}$ film	16.45	5.818	48.8	114	300

range, we added an undamped harmonic oscillator model to Eq. (1):

$$\epsilon(E) = \frac{A_1 E_1^2}{E_1^2 - E^2} \quad (6)$$

In general, we need samples with several crystal orientations to determine the dielectric functions of anisotropic crystals. In the uniaxial ZnO epilayer grown on (0001) sapphire, the optical axis is along the direction normal to the sample surface. In this case, we can easily determine the ordinary and the extraordinary dielectric functions by using a standard ellipsometric configuration [11]. Furthermore, ellipsometric measurements at multiple angles of incidence increase the fitting accuracy.

Figure 1 shows plots of the ellipsometric parameters of ZnO and  $\text{Zn}_{1-x}\text{Mg}_x\text{O}$  ( $x = 0.2, 0.8$ ) thin films grown on (0001) sapphire substrate, and of the curve fits obtained by using multi-layer analysis with a Holden MDF. In the multi-layer modeling, we included the surface roughness by using the EMA. The fit parameters are shown in Table 1. We could fit the anisotropic dielectric functions of the uniaxial ZnO thin film very well [6]. We also assumed an isotropic dielectric function for the  $\text{Zn}_{1-x}\text{Mg}_x\text{O}$  ( $x = 0.2, 0.8$ ) layer. More refined layer modeling includ-

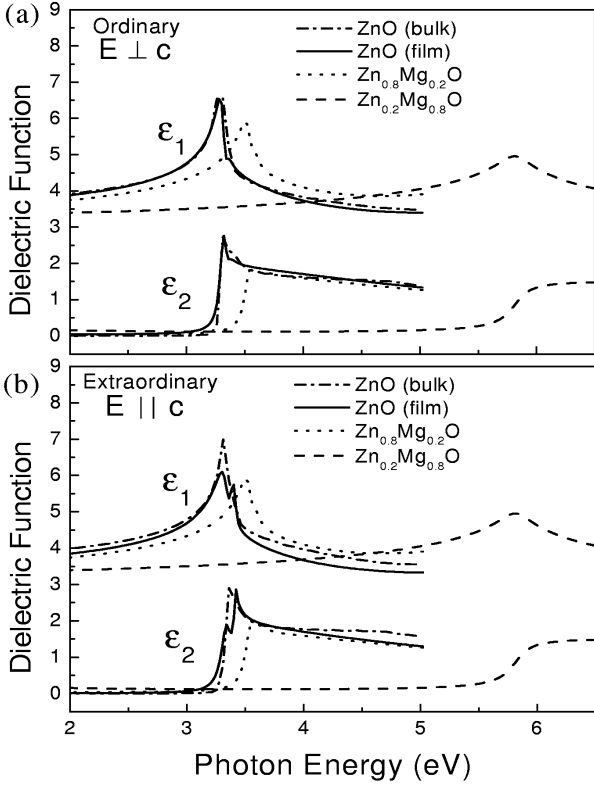


Fig. 2. Plots of the modeled dielectric functions of bulk ZnO, and of the thin films of ZnO,  $\text{Zn}_{0.8}\text{Mg}_{0.2}\text{O}$ , and  $\text{Zn}_{0.2}\text{Mg}_{0.8}\text{O}$ .

ing anisotropic dielectric functions did not improve the fitting in the case of  $\text{Zn}_{1-x}\text{Mg}_x\text{O}$ . We expect that the optical anisotropy of the alloys decreases with increasing Mg composition, because the MgO crystal is isotropic. The fitted thicknesses of the surface roughness layer and the main layer were 11.2 nm and 119.9 nm, respectively, for the ZnO thin film, and 24.7 nm and 344.6 nm for the  $\text{Zn}_{0.8}\text{Mg}_{0.2}\text{O}$  thin film. In the case of the  $\text{Zn}_{0.2}\text{Mg}_{0.8}\text{O}$  thin film, the best fit was achieved using three layers: the roughness layer (27.3 nm), the top layer (13.7 nm), and the main layer (107.9 nm) on sapphire.

Figure 2 is the plot of the fitted dielectric functions of bulk ZnO [6], thin-film ZnO,  $\text{Zn}_{0.8}\text{Mg}_{0.2}\text{O}$ , and  $\text{Zn}_{0.2}\text{Mg}_{0.8}\text{O}$  grown on (0001) sapphire substrates. The fit parameters are shown in Table 1. The first and the second peaks of ZnO thin film were assigned to  $n = 1$  exciton and band-gap peaks, respectively. Note that Jelison and Boatner assigned the second peak to the  $n = 2$  exciton peak, and that Liang and Yoffe assigned it to the exciton-phonon complex [6, 12]. The amplitude of the  $E_0$  gap of thin-film ZnO was similar to that of bulk ZnO. Even under a residual tensile strain, the  $E_0$  band-gap energies of thin-film ZnO were the same as those of bulk ZnO within the experimental errors. The difference in energy between the band-edge energy of the ordinary index ( $E_{0\perp}$ ) and that of the extraordinary in-

dex ( $E_{0\parallel}$ ) was the same as that of bulk ZnO within the errors [6]. The exciton binding energies of ZnO thin film increased in sizable amounts ( $R_{\perp} = 5.8$  meV and  $R_{\parallel} = 21.5$  meV) compared to those of bulk ZnO. The physical origin is not known yet. The increase in the broadening of the ZnO thin film compared to that of bulk ZnO can be attributed to an inhomogeneous strain distribution. The band gap energy of  $\text{Zn}_{0.8}\text{Mg}_{0.2}\text{O}$  increased by 0.2 eV compared to that of the ZnO thin film due to alloying with Mg, whereas the binding energy of  $\text{Zn}_{0.8}\text{Mg}_{0.2}\text{O}$  was similar to that of thin-film ZnO. The increase in the band gap of  $\text{Zn}_{1-x}\text{Mg}_x\text{O}$  with increasing Mg composition is expected because the band gap of MgO is larger than that of ZnO. With increasing Mg composition, the broadening increased. The larger broadening of  $\text{Zn}_{1-x}\text{Mg}_x\text{O}$  is attributed to both alloy-disorder and increased structural inhomogeneity. Presently, we do not have an explanation for the Mg composition dependence of the binding energy of  $\text{Zn}_{1-x}\text{Mg}_x\text{O}$  alloys.

The difference between the band gap energies of the ordinary (electric field ( $E$ )  $\perp$  c axis) and the extraordinary (electric field ( $E$ )  $\parallel$  c axis) dielectric functions was 35 meV and was attributed to the selection rules for interband transitions. The interband transitions are between the  $\Gamma_{7c}$  conduction band and the valence bands. The valence bands of ZnO are split due to the crystal field. However, the valence band ordering of ZnO has been controversial so far. According to the literature, there are two suggestions about the valence-band ordering of ZnO. From top to bottom on the energy scale, the ordering of the valence band has been proposed to be either A( $\Gamma_{9v}$ ), B( $\Gamma_{7v,u}$ ), C( $\Gamma_{7v,l}$ ) (Ref. 6, 13-15), or A( $\Gamma_{7v,u}$ ), B( $\Gamma_{9v}$ ), C( $\Gamma_{7v,l}$ ) (Ref. 5, 16-18). In any case, the oscillator strength of an A exciton is much weaker than those of B and C excitons experimentally [14, 19]. Hence, we assigned  $E_{0\perp}^{ex}$  to the B exciton and  $E_{0\parallel}^{ex}$  to the C exciton from the Figs. 2 (a) and (b), respectively [20, 21].

#### IV. CONCLUSION

We measured the pseudo-dielectric functions of ZnO and  $\text{Zn}_{1-x}\text{Mg}_x\text{O}$  thin films grown on (0001) sapphire substrates. Using a Holden MDF, we fitted the dielectric functions of ZnO and  $\text{Zn}_{1-x}\text{Mg}_x\text{O}$  and determined the critical-point parameters. In the case of a ZnO thin film, we fitted the anisotropic dielectric functions. We compared the critical point parameters of bulk ZnO to those of thin-film ZnO and  $\text{Zn}_{1-x}\text{Mg}_x\text{O}$ . We found that the exciton binding energy associated with the  $E_0$  critical point of the ZnO thin film was larger than that of bulk ZnO.

#### ACKNOWLEDGMENTS

The work of H. Lee was supported in part by the Special Equipment Program of the Korean Basic Science Institute through the Korean Science and Engineering Foundation (KOSEF, R23-2002-000-00006-0). The work of G.-C. Yi was supported by the Advanced Environmental Biotechnology Research Center (No. R11-2003-006).

## REFERENCES

- [1] K. Postava, H. Sueki, M. Aoyama, T. Yamaguchi, Ch. Ino, Y. Igasaki and M. Morie, *J. Appl. Phys.* **87**, 7820 (2000).
- [2] A. Ohtomo, M. Kawasaki, T. Koida, K. Masuchi, H. Koinuma, Y. Sakurai, Y. Yoshida, T. Yasuda and Y. Segawa, *Appl. Phys. Lett.* **72**, 2466 (1998).
- [3] A. Ohtomo, K. Tamura, M. Kawasaki, T. Makino, Y. Segawa, Z. K. Tang, G. K. L. Wong, Y. Matsumoto and H. Koinuma, *Appl. Phys. Lett.* **7**, 2204 (2000).
- [4] W. I. Park, G. C. Yi and H. M. Jang, *Appl. Phys. Lett.* **79**, 2022 (2001).
- [5] H. Yoshikawa and S. Adachi, *Jpn. J. Appl. Phys.* **36**, 6237 (1997).
- [6] G. E. Jellison, Jr. and L. A. Boatner, *Phys. Rev. B* **58**, 3586 (1998).
- [7] J. H. Kang, Y. R. Park and K. J. Kim, *Solid State Commun.* **115**, 127 (2000).
- [8] P. L. Washington, H. C. Ong, J. Y. Dai and R. P. H. Chang, *Appl. Phys. Lett.* **72**, 3261 (1998).
- [9] T. Holden, P. Ram, F. H. Pollak, J. L. Freeouf, B. X. Yang and M. C. Tamargo, *Phys. Rev. B* **56**, 4037 (1997).
- [10] C. Tanguy, *Phys. Rev. Lett.* **75**, 4090 (1995).
- [11] R. M. A. Azzam and N. M. Bashara, *Ellipsometry and Polarized Light* (North-Holland, Amsterdam, 1987).
- [12] W. Y. Liang and A. D. Yoffe, *Phys. Rev. Lett.* **20**, 59 (1968).
- [13] D. C. Reynolds, D. C. Look, B. Jogai, C. W. Litton, G. Cantwell and W. C. Harsh, *Phys. Rev. B* **60**, 2340 (1999).
- [14] B. Gil, *Phys. Rev. B* **64**, 201310 (2001).
- [15] S. F. Chichibu, T. Sota, G. Cantwell, D. B. Eason and C. W. Litton, *J. Appl. Phys.* **93**, 756 (2003).
- [16] D. G. Thomas, *J. Phys. Chem. Solids* **15**, 86 (1960).
- [17] J. J. Hopfield, *J. Phys. Chem. Solids* **15**, 97 (1960).
- [18] W. R. L. Lambrecht, A. V. Rodina, S. Limpijumnong, B. Segall and B. K. Meyer, *Phys. Rev. B* **65**, 075207 (2002).
- [19] S. F. Chichibu, A. Tsukazaki, M. Kawasaki, K. Tamura, Y. Segawa, T. Sota and H. Koinuma, *Appl. Phys. Lett.* **80**, 2860 (2002).
- [20] S. J. So and C. B. Park, *J. Korean Phys. Soc.* **40**, 925 (2002).
- [21] S. J. Kwon, H. J. Lee, Y. W. Seo and H. S. Jeong, *J. Korean Phys. Soc.* **43**, 709 (2003).